This is the accepted version of the following article: Orsini F, Santacroce M, Cremona A, Gosvami NN, Lascialfari A, Hoogenboom BW. 2014. Atomic force microscopy on plasma membranes from Xenopus laevis oocytes containing human aquaporin 4. *J. Mol. Recognit.* **27**: 669–675, which has been published in final form at http://dx.doi.org/10.1002/jmr.2390 .

Atomic force microscopy on plasma membranes from *Xenopus laevis* oocytes containing human aquaporin 4

Francesco Orsini[a,*], Massimo Santacroce[b], Andrea Cremona[b], Nitya N. Gosvami[c,d,†], Alessandro Lascialfari[a], Bart W. Hoogenboom[c,e]

[a] *Dipartimento di Fisica, Università degli Studi di Milano, via Celoria 16, 20133 Milano, Italy*

[b] *Dipartimento di Scienze Farmacologiche e Biomolecolari, Università degli Studi di Milano, via Trentacoste 2, 20134 Milano, Italy*

[c] *London Centre for Nanotechnology, University College London, 17-19 Gordon Street, London WC1H 0AH, United Kingdom*

[d] *Department of Chemistry, University College London, 20 Gordon Street, London WC1H 0AJ, United Kingdom*

[e] *Department of Physics and Astronomy, University College London, Gower Street, London WC1E 6BT, United Kingdom*

*Corresponding author:
Francesco Orsini, Dipartimento di Fisica, Università degli Studi di Milano, via Celoria 16, 20133 Milano, Italy. E-mail: francesco.orsini@unimi.it

† Present address: Department of Mechanical Engineering and Applied Mechanics, University of Pennsylvania, 229 Towne, 220 S. 33rd St., Philadelphia, PA 19104-6315 USA.

Abstract

Atomic force microscopy (AFM) is a unique tool for imaging membrane proteins in near-native environment (embedded in a membrane and in buffer solution) at ~1 nm spatial resolution. It has been most successful on membrane proteins reconstituted in two-dimensional (2D) crystals and on some specialized and densely packed native membranes. Here we report on AFM imaging of purified plasma membranes from *Xenopus laevis* (*X. laevis*) oocytes, a commonly used system for the heterologous expression of membrane proteins. Isoform M23 of human aquaporin 4 (AQP4-M23) was expressed in the *X. laevis* oocytes following their injection with AQP4-M23 cRNA. AQP4-M23 expression and incorporation in the plasma membrane were confirmed by the changes in oocyte volume in response to applied osmotic gradients. Oocyte plasma membranes were then purified by ultracentrifugation on a discontinuous sucrose gradient and the presence of AQP4-M23 proteins in the purified membranes was established by Western Blotting analysis. Compared to membranes without over-expressed AQP4-M23, the membranes from AQP4-M23 cRNA injected oocytes showed clusters of structures with lateral size of about 10 nm in the AFM topography images, with a tendency to four-fold symmetry as may be expected for higher-order arrays of AQP4-M23. In addition, but only infrequently, AQP4-M23 tetramers could be resolved in two-dimensional (2D) arrays on top of the plasma membrane, in good quantitative agreement with TEM analysis and the current model of AQP4. Our results show the potential as well as the difficulties of AFM studies on cloned membrane proteins in native eukaryotic membranes.

Keywords

Atomic Force Microscopy; *Xenopus laevis* oocyte; aquaporin 4; membrane proteins; heterologous expression.

1. Introduction

Atomic Force Microscopy (AFM) is a powerful technique to obtain three-dimensional images with nanometer resolution of biological samples under physiological conditions (Bippes and Muller, 2011; Casuso *et al.*, 2011; Orsini *et al.*, 2012). In particular, AFM allows to visualize and manipulate membrane proteins in their native state without the necessity to solubilise them. Impressive images of membrane proteins in natural aqueous environment have been recorded, and a quantitative interpretation of the data acquired using AFM has become possible (Muller and Engel, 2008; Sturgis *et al.*, 2009). This includes protein surface density, local inhomogenities as well as various topographic and structural arrangements in a native environment (Muller *et al.,* 2006; Bippes and Muller, 2011). However, for highest spatial resolution on membrane proteins, the technique usually relies on protein purification and subsequent reconstitution in artificial membranes, and preferably in 2D crystals, at the exception of AFM experiments on membrane proteins in some densely packed and/or specialized native membranes.

Xenopus laevis (*X. laevis*) oocyte plasma membranes represent a much more general system for imaging membrane proteins, as *X. laevis* oocytes are widely used for the cloning and characterization of heterologous proteins in many fields of life sciences from physiology to molecular biology. In fact, *X. laevis* oocytes are able to efficiently translate exogenous mRNA into proteins upon injection of the corresponding mRNA. More particularly, the use of *X. laevis* oocytes has been extremely fruitful in the expression of receptor, channel and transporter proteins, to subsequently take advantage of sensitive techniques such as electrophysiology and radiotracer uptake as extensively reported in the literature (Cucu *et al.*, 2004; Mari *et al.*, 2006; Musa-Aziz *et al.*, 2010). Compared to those techniques, the advantage of AFM lies in its ability to obtain nanometer-scale and time-lapse information on the submolecular structure and supramolecular assembly of functional membrane proteins, e.g., visualizing conformational changes (Scheuring *et al.,* 2006; Mari *et al.*, 2011; Picas *et al.*, 2013). The scope for such AFM experiments would be greatly enlarged if AFM could image heterologous membrane proteins with well-controlled orientation in *X. laevis* oocyte plasma membranes. This would also facilitate the comparison of functional characterization by, e.g., patch-clamp techniques, to nanometer-scale structural information on the same system.

Over the past years, there have been several AFM studies of the plasma membrane in *X. laevis* oocytes (Lau *et al.*, 2002; Schillers *et al.*, 2000, 2004, 2008; Orsini *et al*., 2010, Santacroce *et al.*, 2013), though thus far of insufficient resolution to identify native or heterologous membrane proteins based on their topography in the membrane. Here we report on further steps in this direction.

In this paper, AFM imaging has been applied to the study of *X. laevis* oocyte plasma membranes purified by an ultracentrifugation process on a discontinuous sucrose gradient, and expressing the isoform M23 of human aquaporin 4 (AQP4-M23). AQP4-M23 has been chosen as a model system for our method because it has been shown to form orthogonal arrays of intramembraneous particles (Neely *et al.*, 1999; Furman *et al.*, 2003; Crane *et al.*, 2009), where each intramembraneous particle corresponds to an individual AQP4-M23 tetramer. This lattice formation should facilitate imaging and identification of AQP4-M23 by AFM, and possibly comparison to high-resolution AFM studies of aquaporin proteins reconstituted in 2D crystals (Scheuring *et al.,* 2000; Fotiadis *et al.*, 2000; Fotiadis *et al.*, 2002) and in more specialized native membranes (Buzhynskyy *et al.,* 2007; Scheuring *et al.,* 2007; Rico *et al.*, 2013).

If successful, the imaging of heterologous proteins in *X. laevis* oocyte membranes will enable scientists to exploit the above-mentioned advantages of AFM for a much wider range of membrane proteins than is currently possible, without the need for protein purification and crystallization.

2. Materials and methods

2.1 Oocyte preparation

The oocytes were isolated from mature *X. laevis* female frogs, and manually defolliculated after treatment with collagenase A (1 mg/mL; Roche, Germany) in the Ca^{2+}-free ORII buffer (82.5 mM NaCl, 2 mM KCl, 1 mM $MgCl_2$, and 5 mM Hepes/Tris, pH 7.5) for 30 minutes at room temperature. Selected V and VI stadium defolliculated oocytes were maintained at 16 °C in Barth's medium (88 mM NaCl, 1 mM KCl, 0.82 mM $MgSO_4$, 0.41 mM $CaCl_2$, 0.33 mM $Ca(NO_3)_2$, and 10 mM Hepes/Tris, pH 7.5) supplemented with 0.005% gentamycin sulfate and 2.5 mM pyruvic acid.

2.2 cRNA oocyte injection

The complementary RNA (cRNA) for human aquaporin 4 (AQP4) was isolated from the oocyte expression vector pGEMHE containing AQP4 cDNA (isoform M23) that has been generously provided by P. Agre (Departments of Biological Chemistry and Medicine, Johns Hopkins University School of Medicine, Baltimore, MD, USA). Briefly, after linearization by *Xba1* digestion, the cDNA was *in vitro* capped and transcribed with T7 RNA polymerase (Promega). Template plasmide was removed by digestion with RNase-free DNase I. cRNA was purified by phenol/chloroform extraction followed by precipitation with 0.5 volumes of 7.5 M ammonium acetate and 2.5 volumes of ethanol to remove unincorporated trinucleotides, then solubilised in RNase-free water, aliquoted and stored at – 80 °C. Integrity of the transcript was checked by denaturated agarose gel electrophoresis.

For the expression of AQP4-M23 on oocyte plasma membrane, 12.5 ng of cRNA in 50 nL of RNase-free water were injected at the animal-vegetal interface of healthy looking V and VI stage defolliculated oocytes using a manual microinjection system (Drummond, Broomall, PA, USA). Injected oocytes were incubated at 18 °C for 3-4 days in Barth's solution supplemented with 50 µg/ml gentamicin sulfate and 2.5 mM sodium pyruvate. Plasma membrane samples of injected oocytes were purified and prepared for AFM imaging following the under described procedures.

2.3 Purification of oocyte plasma membrane by ultracentrifugation

About 100-200 V- and VI-stage defolliculated, AQP4-M23 cRNA injected oocytes were homogenized in oocyte homogenization buffer (OHB) (250 mM sucrose, 5 mM $MgCl_2$, 10 mM Hepes/Tris, pH 7.5; 10 µL per oocyte) by several cycles of pipetting. Homogenates were centrifuged at 500g for 5 minutes at 4°C. Lipids floating on the liquid surface were discarded, and the supernatant was recovered (about 1 mL). The pellet was resuspended in 1 mL of OHB and homogenized as above before centrifugation at 500g for 5 minutes at 4°C. The supernatant was recovered (about 500 µL) and combined with the first one. A volume of 1.5 mL of the supernatant was loaded on bottom of a discontinuous sucrose gradient composed of 80% sucrose in TNE buffer (10 mM Tris/HCl, 150 mM NaCl, pH 7.4) (1.5 mL), 35% sucrose in TNE (4 mL), 10% sucrose in TNE (4 mL) and centrifuged at 30,000g for 3 hours at 4°C in a swinging bucket rotor (Beckman). At the end of the ultracentrifugation process a major membrane band was clearly visible at the interface between 35% and 10% sucrose. The band was then collected and stored until use at -20°C.

2.4 Sample preparation for AFM imaging

Purified membranes were diluted 1:20 in adsorption buffer (150 mM KCl, 250 mM $MgCl_2$, 10 mM Tris/HCl, pH 7.5). Before sample deposition, the mica support was immersed in 100 µL of adsorption buffer for 1 minute to facilitate the membrane adhesion. Subsequently, the buffer was removed and 50 µL of the membrane suspension were floated on the mica surface. After 10 minutes of adsorption, the sample was gently rinsed three times with 50 µL of recording buffer (150 mM KCl, 10 mM Hepes/Tris, pH 7.5) to remove membranes that had not been adsorbed to the support. Finally the buffer was removed, leaving just sufficient buffer to keep the sample hydrated, and a drop of 70 µL of recording buffer was placed on the mica support before AFM imaging.

2.5 Western blot analysis for AQP4-M23

Purified oocyte membranes were separated by SDS-PAGE (10% polyacrylamide gel) and transferred onto a polyvinylidene difluoride (PVDF) membrane overnight then blocked in blocking

buffer consisting of 5% (w/v) dried non-fat milk in Tris-buffered saline (T-TBS: 10 mM Tris/HCl, pH 7.5, 150 mM NaCl, 0.1% (v/v) Tween®20) at room temperature for 1 hour. The membrane was then incubated at room temperature for 2 hours with primary antibodies against AQP4-M23 (Santa Cruz Biotechnology, USA) diluted 1:200 in blocking buffer. The blots were washed with T-TBS and then incubated with the proper secondary antibody in blocking buffer at room temperature for 1 hour. The protein bands were visualized using enhanced chemiluminescence (ECL) reagents (PerkinElmer, USA).

2.6 Volumetric analysis of oocyte osmotic swelling

Groups of 6-10 defolliculated, AQP4-M23 cRNA injected oocytes were transferred from a Petri dish containing the Barth's solution (207 mOsm) to a Petri dish containing a 40 mOsm (ΔmOsm = 167) hypoosmotic buffer (16.25 mM NaCl, 5 mM Hepes, 2.5 mM Trizma base, pH 7.5). The experiment was performed at 25 °C.

8 bit grey scale pictures of oocyte groups were collected every 2, 3, 10 or 30 seconds for a total time varying from 200 to 600 seconds using a 5.1 megapixels CCD sensor video camera (Bel, Italy) connected to a stereomicroscope, using BEL Eurisko software (version 2.9). Two assumptions were required for the analysis: the oocytes had to be spherical and they were focused at the equator. Thus the diameter determined in the two-dimensional image equals that of the sphere (Zeuthen *et al.*, 1997). An oocyte viewed in brightfield microscopy is a black circular area and its area value in pixel (cross section, CS) allows the oocyte relative volume (V_t / V_0) to be derived using the relationship $V_t / V_{t0} = (CS_t / CS_{t0})^{3/2}$. Thus, given the above assumptions, the V_t / V_{t0} value depends only on the CS values. CS values were computed at each acquisition time using ImageJ software (http://rsbweb.nih.gov/ij).

2.7 Atomic Force Microscopy

AFM imaging was performed using Nanoscope Multimode IIId and IV AFM systems (Bruker, Santa Barbara, CA, USA), as well as on a home-built system for frequency-modulation (FM) AFM (Hoogenboom *et al.*, 2006; Hoogenboom *et al.*, 2007; Khan *et al.*, 2010). All AFM experiments were carried out in a recording buffer containing 150 mM KCl, 10 mM Hepes/Tris, pH 7.5. Tapping-mode AFM images were collected using the RMS amplitude of the cantilever as the feedback signal for the vertical sample position. The mica support (Ted Pella, CA, USA) was glued to a Teflon layer which in turn was glued to a metal disk that was magnetically fixed to the AFM sample holder. Rectangular silicon nitride probes with nominal spring constant around 2.5 N/m (NSG01, NT-MDT, Russia) and cantilever length of 120 μm were used for the tapping-mode

imaging. The cantilever resonance frequency was about 30 kHz. The RMS free amplitude of the cantilever was approximately 15 nm and the relative set-point above 95% of the free amplitude. FM-AFM was carried out with PPP-NCH silicon probes with nominal spring constant of 40 N/m, and resonance frequency of ~150 kHz in liquid (Nanosensors, Switzerland). Images were recorded at ~1 Hz line rate and a resolution of 512x512 pixels per image was chosen. AFM images were subject to a line-by-line subtraction of linear background ("flattening"), to eliminate sample tilt from the images and correct for step-wise changes between individual scan lines.

3. Results

In the present work, complementary RNA (cRNA) was synthesized in vitro from cDNA clones of human aquaporin 4, isoform M23 (AQP4-M23) and was then microinjected into defolliculated *X. laevis* oocytes for functional expression. To verify the functional expression of AQP4-M23 in the oocyte plasma membrane, the membrane water permeability of oocytes was measured in a hypoosmotic buffer by means of video microscopy analysis, three days after the microinjection (see Materials and methods section). Figure 1a reports the relative volume increase (V/V_0) versus time for control and AQP4-M23 expressing oocytes (injected with a cRNA concentration of about 0.3 µg/µl), incubated in a hypo-osmotic buffer (40 mOsm). The data represent the mean of three independent experiments.

The volumetric analysis clearly shows that *X. laevis* oocytes have low intrinsic water permeability and that AQP4-M23 expressing oocytes have a water permeability significantly higher than control oocytes, thus confirming the presence of AQP4-M23 proteins in the oocyte plasma membrane in their functional form.

In addition, to better characterize the AQP4-M23 expression and to find out protein over-expression conditions, the volumetric analysis was also performed on oocytes injected with different concentrations of cRNA, namely 0.1, 0.25 and 0.5 µg/µl. Figure 1b reports the mean slope of the relative volume versus time curves calculated in the first 30 seconds, as a function of the cRNA concentration. As expected, there is the correlation between the cRNA concentration and the level of protein expression and AQP4-M23 activity, though this is only obvious until ~ 0.3 µg/µl. The data for 0.5 µg/µl cRNA indicate that the water permeability slightly decreases in comparison to the one observed in oocytes injected with a lower concentration. This suggests that a saturation level was reached.

From these experimental data, we deduced that the highest expression of functional AQP4-M23 was obtained by injecting oocytes with a cRNA concentration of about 0.3 µg/µl. This concentration was therefore used to prepare the membrane samples for the AFM experiments described below.

The presence of AQP4-M23 proteins in purified oocyte plasma membrane samples was verified, before performing AFM imaging, by SDS-PAGE and Western blot analysis. The biochemical assay reported in Figure 1c shows the presence of a band around 30 kDa for oocytes that have been injected with an AQP4-M23 cRNA concentration of 0.3 μg/μl. This band corresponds to the molecular weight of a single monomeric unit of an AQP4-M23 tetramer. It is absent in the control oocytes. Moreover, highest AQP4-M23 content was found in oocytes injected with a cRNA concentration of 0.3 μg/μl in comparison with oocytes injected with a cRNA concentration of 0.1 μg/μl as expected by the volumetric analysis data.

AFM imaging of *X. laevis* oocyte plasma membrane was performed on membrane specimens purified according to the sample preparation protocol described in the Materials and methods section and discussed in detail elsewhere (Santacroce *et al.*, 2013). Briefly, this method is based on the purification of functional plasma membrane of *X. laevis* oocytes by ultracentrifugation on a discontinuous sucrose gradient. After their deposition on a mica support, the membranes are imaged in buffer solution by AFM.

AFM imaging performed on native *X. laevis* oocyte membranes showed large and planar membrane patches adhered to the mica support, with lateral sizes of a few microns and an height of about 4-5 nm as expected for a membrane lipid bilayer (see Figure 2a and Santacroce *et al.*, 2013). On higher magnification, some membrane patches showed roughly spherical, isotropic structures with lateral sizes of about 10 nm and protruding from the membrane surface by about 1-2 nm as reported in Figure 2b.

On the purified plasma membranes obtained from oocytes injected with an AQP4-M23 cRNA concentration of 0.3 μg/μl, AFM topography images showed a situation comparable to the one observed on native samples, namely planar membrane patches with lateral sizes, typically, of a few microns and heights of about 5 nm (see Figure 3a). While some membrane patches had an apparently smooth surface, others showed larger surface roughness.

On higher magnification, we observed protrusions from the membrane with a diameter of about 10 nm and protruding by about 1 nm from the membrane surface as reported in Figure 3b. Interestingly, and unlike the protrusions observed in native membranes (Figure 2b), these structures often appeared clustered and arranged according to a square motif. While such a motif could also arise due to a tip-artifact where the same pattern in repeated in a stamp-like manner, we note that the orientation of the apparent square symmetry is not identical for different clusters in the image (Figures 3c-e). Since this tendency to a four-fold symmetry has only been observed in membrane samples prepared from transfected oocytes (cf. membranes from untransfected oocytes in Figure 2b and also Schillers *et al.*, 2000; Lau *et al.*, 2002; Orsini *et al.*, 2010, Santacroce *et al.*, 2013), we

tentatively interpret the visualized structures as higher-order orthogonal arrays of AQP4-M23 proteins. Higher spatial resolution remained elusive on these membranes though, preventing a more definite identification.

In a rare occasion, for a sample of plasma membrane obtained by *X. laevis* oocytes injected with cRNA for the M23 isoform of AQP4, a much clearer signature of AQP4-M23 could be found. Figure 4a reveals a 4 nm high plateau on top of the membrane, with a square lattice structure of identical dimensions as observed by electron microscopy on a freeze fracture preparation (see inset of Figure 4b – identical to the inset in 3f – from Furman *et al.*, 2003). In particular, an AFM topography image collected in this region and reported in Figure 4b shows a square lattice array with uniform lattice spacing of 4-5 nm. These particles appear to be arranged along two orthogonal axes of symmetry giving them a checkerboard appearance. The size of the single particles, in the range of 4-5 nm, the angles and the lattice spacing as measured by AFM topography images (λ = 4.7 ± 0.5 nm, Figure 4c) are compatible with the AQP4-M23 tetramer supramolecular assembly with 4-6 nm periodicity as observed in cell membranes by electron microscopy (Furman *et al.*, 2003; Crane *et al.*, 2009; Fenton *et al.*, 2010), and similar in appearance to the cytoplasmic surface of reconstituted AQP0, a homologue of AQP4 (Figure 4e, from Fotiadis *et al*, 2000).

4. Discussion

Compared to earlier AFM experiments on *X. laevis* oocyte plasma membranes without over-expression of heterologous proteins (Schillers *et al.*, 2000; Lau *et al.*, 2002; Orsini *et al*., 2010; Santacroce *et al.*, 2013), the current study displays various smaller complexes of intramembraneous particles arranged according to a square motif, in various orientations, as well as the presence of a lattice on top of the plasma membrane with lattice constants as expected for larger arrays of AQP4-M23 tetramers.

The AFM images thus contain signatures of the presence of AQP4-M23, in agreement with the volumetric and biochemical analyses that clearly demonstrate the over-expression of AQP4-M23 in the oocyte plasma membrane. Since *X. laevi*s oocytes are commonly used for heterologous expression of membrane proteins, the here outlined procedures point to a promising route for study of tertiary and quaternary structure of cloned membrane proteins by AFM.

However, there also remain several obstacles to such an approach, as apparent from the results presented here. Smaller clusters of intramembraneous particles can be observed regularly, though not at sufficient spatial resolution to identify individual aquaporin tetramers (Figure 3). High spatial resolution should be more readily obtainable on larger arrays of proteins in the membrane, since such arrays provide stabilisation against thermal fluctuations and the forces exerted by the AFM tip.

Unfortunately AFM on the purified plasma membranes only rarely shows the regular arrays of aquaporin tetramers (as expected for AQP4-M23), and not in, but on the plasma membrane (Figure 4).

Additional complications arise because – as can be inferred from Figure 1 – the over-expression of AQP4-M23 cannot be arbitrarily increased to achieve higher packing densities. The oocyte membranes are therefore rather different from reconstituted or specialised bacterial membranes in that the packing density of the membrane proteins is not as favourable to high-resolution AFM imaging.

In eukaryotic membranes such as studied here, protein/lipid ratio is usually rather low (1:1 weight ratio – (Muller *et al.*, 2008 and references therein)), which may also leave the membranes less stable during the processes of purification and deposition of the membranes on mica, and further work would be needed to establish structural changes in the membrane resulting from these processes.

5. Conclusions

In this work AFM has been applied to the study of the plasma membrane of *X. laevis* oocytes that express an heterologous membrane protein, where the isoform M23 of the human aquaporin 4 (AQP4-M23) was selected as a model system for our method.

The AQP4-M23 cRNA was injected in the oocyte cytoplasm and volumetric analysis experiments verified the functional expression and incorporation of AQP4-M23 in the plasma membrane. The oocyte plasma membranes were then purified by ultracentrifugation and Western Blotting analysis proved the presence of AQP4-M23 in the purified samples. AFM topography images showed structures with a diameter of about 10 nm, arranged according to a square motif and protruding from the membrane surface by about 1 nm. These structures have been observed only in membrane samples prepared from transfected oocytes and may be interpreted as higher-order orthogonal arrays of AQP4-M23. Moreover, our AFM experiments have shown a well defined, square-lattice arrangement with surface density and lattice constants of identical dimensions as the AQP4-M23 arrays that were observed by electron microscopy. In the absence of further biochemical identification, based on the comparison with the higher-order structures of AQP4-M23 which stand out as square arrays in freeze fracture preparation (Furman *et al.*, 2003; Crane *et al.*, 2009; Fenton *et al.*, 2010) and the consideration that square lattice arrays of intramembraneous particles were found only in AQP4-M23 transfected *X. laevis* oocytes, we identify the particles in the observed lattice on the oocyte plasma membrane as individual AQP4-M23 tetramers.

These results thus represent the first observation by AFM of heterologously expressed membrane proteins in samples of *X. laevis* oocyte plasma membranes, implying a possible route for AFM studies on cloned membrane proteins without the need for crystallization, with the potential of *in-situ* characterization of the response of membrane proteins to, e.g., ligands and drugs added to the solution. That said, the nanometer-scale characterization and identification of individual AQP4-M23 proteins thus far remains elusive, indicating that there are still significant hurdles to take for this to become mainstream and widely applicable in a wider biological context.

Acknowledgments

AQP4-M23 clone was a generous gift of Prof. Peter Agre, Departments of Biological Chemistry and Medicine, Johns Hopkins University School of Medicine, Baltimore, MD, USA. This work was supported by a Royal Society International Joint Project Grant (2009/R1).

References

Bippes CA, and Muller DJ. 2011. High-resolution atomic force microscopy and spectroscopy of native membrane proteins. *Rep. Prog. Phys.* **74**: 086601.

Buzhynskyy N, Girmens JF, Faigle W, and Scheuring S. 2007. Human Cataract Lens Membrane at Subnanometer Resolution. *J. Mol. Biol.* **374**: 162–169.

Casuso I, Rico F, and Scheuring S. 2011. Biological AFM: where we come from – where we are – where we may go. J. *Mol. Recognit.* **24**: 406–413.

Crane JM, Bennett JL, and Verkman AS. 2009. Live cell analysis of aquaporin-4 M1/M23 interactions and regulated orthogonal array assembly in glial cells. *J. Biol. Chem.* **284**: 35850-35860.

Cucu D, Simaels J, Jans D, Van Driessche W. 2004. The transoocyte voltage clamp: a non-invasive technique for electrophysiological experiments with *Xenopus laevis* oocytes. *Pflügers Arch.* **447**: 934–942.

Fenton RA, Moeller HB, Zelenina M, Snaebjornsson MT, Holen T, MacAulay N. 2010. Differential water permeability and regulation of three aquaporin 4 isoforms. *Cell. Mol. Life Sci.* **67**: 829-840.

Fotiadis D, Hasler L, Muller DJ, Stahlberg H, Kistler J, and Engel A. 2000. Surface Tongue-and-groove Contours on Lens MIP Facilitate Cell-to-cell Adherence. *J. Mol. Biol.* **300:** 779–789.

Fotiadis D, Suda K, Tittmann P, Jeno P, Philippsen A, Muller DJ, Gross H, and Engel A. 2002. Identification and Structure of a Putative Ca^{2+}-binding Domain at the C Terminus of AQP1. *J. Mol. Biol.* **318:** 1381–1394.

Furman CS, Gorelick-Feldman DA, Davidson KGV, Yasumura T, Neely JD, Agre P, and Rash JE. 2003. Aquaporin-4 square array assembly: Opposing actions of M1 and M23 isoforms. *Proc. Natl. Acad. Sci. U.S.A.* **100**: 13609-13614.

Hoogenboom BW, Hug HJ, Pellmont Y, Martin S, Frederix PLTM, Fotiadis D, EngelA. 2006. Quantitative dynamic-mode scanning force microscopy in liquid. *Appl. Phys. Lett*. **88**: 193109.

Hoogenboom BW, Suda K, Engel A, Fotiadis D. 2007. The supramolecular assemblies of voltage-dependent anion channels in the native membrane. *J. Mol. Biol.* **370**: 246-255.

Khan Z, Leung C, Tahir BA, Hoogenboom BW. 2010. Digitally tunable, wide-band amplitude, phase, and frequency detection for atomic-resolution scanning force microscopy. *Rev. Sci. Instrum.* **81**: 073704.

Lau JM, You HX, Yu L. 2002. Lattice-Like Array Particles on Xenopus oocyte Plasma Membrane. *Scanning* **24**: 224–231.

Mari SA, Soragna A, Castagna M, Santacroce M, Perego C, Bossi E, Peres A, Sacchi VF. 2006. Role of the conserved glutamine 291 in the γ-aminobutyric acid transporter rGAT-1. *Cell. Mol. Life Sci.* **63**: 100–111.

Mari SA, Pessoa J, Altieri S, Hensen U, Thomas L, Morais-Cabral JH, Muller DJ. 2011. Gating of the MlotiK1 potassium channel involves large rearrangements of the cyclic nucleotide-binding domains. *Proc. Natl. Acad. Sci. U.S.A.* **108**: 20802-20807.

Muller DJ, Sapra KT, Scheuring S, Kedrov A, Frederix PL, Fotiadis D, and Engel A. 2006. Single-molecule studies of membrane proteins. *Curr. Opin. Struc. Biol.* **16**: 489–495.

Muller DJ, Engel A. 2008. Strategies to prepare and characterize native membrane proteins and protein membranes by AFM. *Current Opinion in Colloid & Interface Science* **13**: 338-350.

Muller DJ, Wu N, and Palczewski K. 2008. Vertebrate Membrane Proteins: Structure, Function, and Insights from Biophysical Approaches. *Pharmacological Reviews* **60**: 43-78.

Musa-Aziz R, Boron WF, Parker MD. 2010. Using fluorometry and ion-sensitive microelectrodes to study the functional expression of heterologously-expressed ion channels and transporters in *Xenopus* oocytes. *Methods* **51**: 134–145.

Neely JD, Christensen BM, Nielsen S, and Agre P. 1999. Heterotetrameric composition of aquaporin-4 water channels. *Biochemistry* **38**: 11156-11163.

Orsini F, Santacroce M, Arosio P, Sacchi VF. 2010. Observing *Xenopus laevis* oocyte plasma membrane by atomic force microscopy. *Methods* **51**: 106–113.

Orsini F, Cremona A, Arosio P, Corsetto PA, Montorfano G, Lascialfari A, Rizzo AM. 2012. Atomic Force Microscopy imaging of lipid rafts of human breast cancer cells. *Biochim. Biophys. Acta – Biomembranes* **1818**: 2943-2949.

Picas L, Rico F, Deforet M, Scheuring S. 2013. Structural and Mechanical Heterogeneity of the Erythrocyte Membrane Reveals Hallmarks of Membrane Stability. *ACS Nano* **7**: 1054-1063.

Rico F, Picas L, Colom A, Buzhynskyy N, and Scheuring S. 2013. The mechanics of membrane proteins is a signature of biological function. *Soft Matter* **9**: 7866–7873.

Santacroce M, Daniele F, Cremona A, Scaccabarozzi D, Castagna M, and Orsini F. 2013. Imaging of *Xenopus laevis* oocyte plasma membrane in physiological-like conditions by Atomic Force Microscopy. *Microsc. Microanal.* **19**: 1358–1363.

Scheuring S, Tittmann P, Stahlberg H, Ringler P, Borgnia M, Agre P, Gross H, and Engel A. 2000. The Aquaporin Sidedness Revisited. *J. Mol. Biol.* **299**: 1271–1278.

Scheuring S, Goncalves RP, PrimaV, and Sturgis JN. 2006. The photosynthetic apparatus of Rhodopseudomonas palustris: Structures and organization. *J. Mol. Biol.* **358**: 83–96.

Scheuring S, Buzhynskyy N, Jaroslawski S, Goncalves RP, Hite RK, Walz T. 2007. Structural models of the supramolecular organization of AQP0 and connexons in junctional microdomains. *J. Struct. Biol.* **160**: 385–394.

Schillers H, Danker T, Schnittler HJ, Lang F, Oberleithner H. 2000. Plasma membrane plasticity of Xenopus laevis oocyte imaged with atomic force microscopy. *Cell Physiol Biochem* **10**: 99–107.

Schillers H, Shahin V, Albermann L, Schaffer C, Oberleithner H. 2004. Imaging CFTR: A tail to tail dimer with a central pore. *Cell Physiol Biochem* **14**: 1–10.

Schillers H. 2008. Imaging CFTR in its native environment. *Pflugers Arch* **256**: 163–177.

Sturgis JN, Tucker JD, Olsen JD, Hunter CN, and Niederman RA. 2009. Atomic Force Microscopy studies of native photosynthetic membranes. *Biochemistry* **48**: 3679-3698.

Zeuthen T, Meinild AK, Klaerke DA, Loo DD, Wright EM, Belhage B, Litman T. 1997. Water transport by the Na+/glucose cotransporter under isotonic conditions. *Biol. Cell* **89**: 307–312.

.

Figure Captions

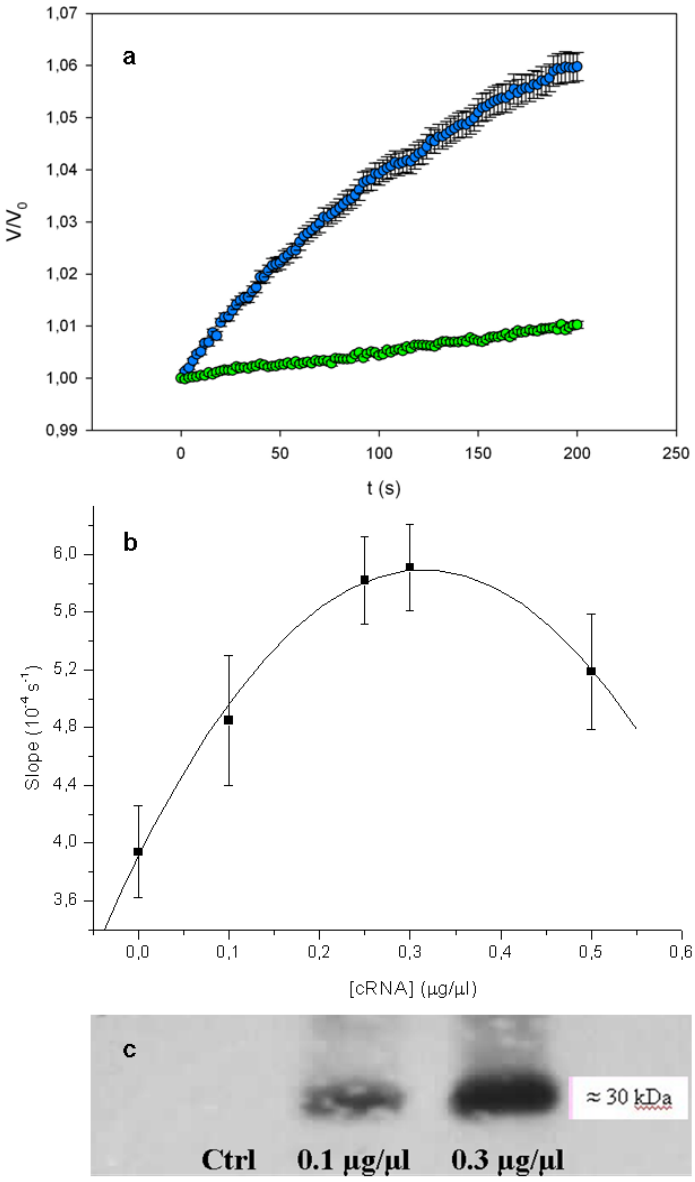

Figure 1.

(a) V/V_0 time course of control oocytes (green) and oocytes (blue) that had been injected with an AQP4-M23 cRNA concentration of 0.3 µg/µl, on incubation in a hypoosmotic buffer (40 mOsm). V/V_0 data were calculated as mean ± standard deviation for 15 oocytes.

(b) Slope of the V/V_0 time course of AQP4-M23 expressing oocytes versus the concentration of injected cRNA. V/V_0 data were calculated as mean ± standard deviation of 15 oocytes. The solid line is a guide to the eye.

(c) Detection of AQP4-M23 proteins in purified *X. laevis* oocyte plasma membranes. Equal volumes for control oocytes (Ctrl) and AQP4-M23 cRNA injected oocytes (0.1 µg/µl and 0.3 µg/µl) were analyzed by Western blot with anti-AQP4-M23.

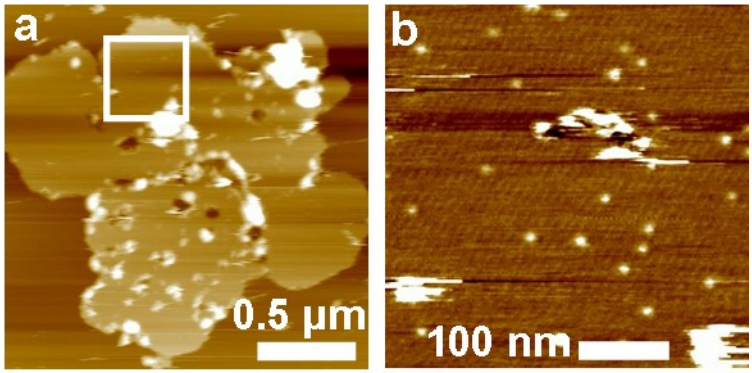

Figure 2.

AFM topography images of a native *X. laevis* oocyte plasma membrane (i.e., without AQP4-M23 cRNA injection) collected in liquid buffer. (**a**) Large-scale image of a sample area that is covered by a patch of plasma membrane. Vertical (false-color) scale: 25 nm. (**b**) Magnification of the area marked by the white square in (a). Vertical scale: 3 nm.

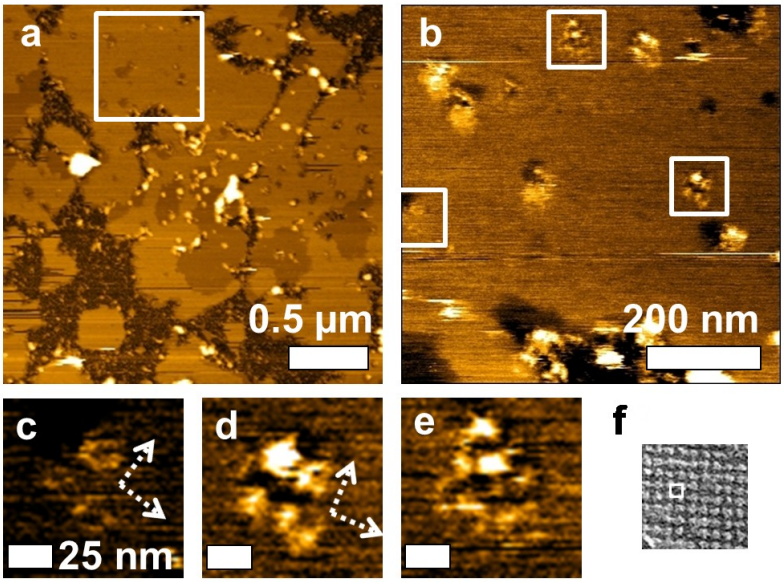

Figure 3.

AFM topography image of *X. laevis* oocyte plasma membrane expressing AQP4-M23 proteins collected in liquid buffer. (**a**) Large-scale image of a sample area that is largely covered by plasma membrane. (**b**) Magnification of the area marked by the white square in (a). (**c-e**) Magnifications of the areas marked by the white squares in (b), showing protrusions in various assemblies and orientations, with arrows in (c) and (d) indicating suggested axes of square-like motifs. Scale bars are 25 nm. (**f**) AQP4-M23 lattice, as measured by electron microscopy (Furman *et al.*, 2003), on the same scale. Vertical (false-color) scales: (a) 15 nm; (b) 2 nm; (c-e) 1 nm.

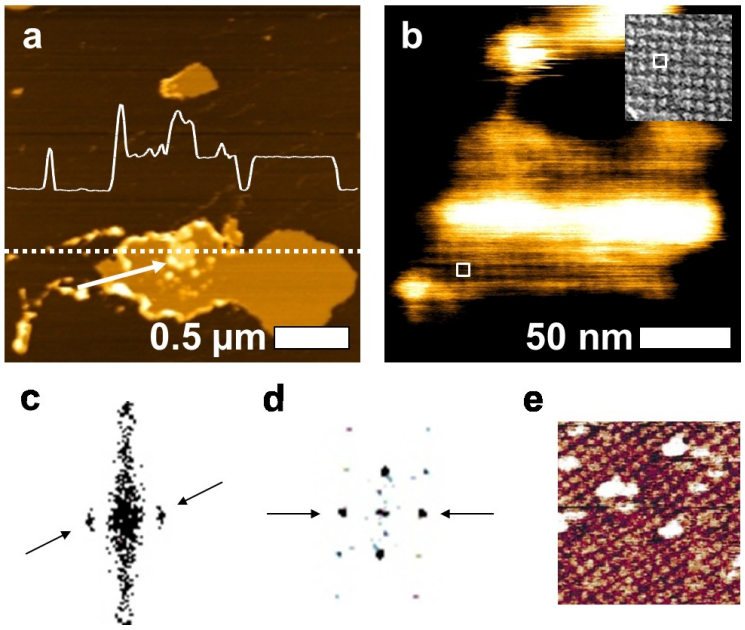

Figure 4.

AFM topography image of *X. laevis* oocyte plasma membrane expressing AQP4-M23 proteins collected in liquid buffer. (**a**) Mica substrate partially covered with the oocyte plasma membrane (4 nm high). The white line indicates the profile measured along the dotted line. Vertical scale: 15 nm. (**b**) Magnification of the 4 nm high patch on top of the plasma membrane, as marked by the arrow in (a). The inset corresponds to an electron microscopy by Furman *et al.*, 2003. Vertical scale 2 nm. The inset reproduces the electron microscopy image of Figure 3f on a matching scale. (**c**) Two-dimensional power spectrum of (b), showing two peaks (see arrows) corresponding to a lattice unit vector of $\lambda = (4.7 \pm 0.5)$ nm. (**d**) As (c), for the electron microscopy in the inset of (b), with reported periodicity between 4-6 nm. (**e**) AFM topography (100 x 100 nm^2) of the cytoplasmic surface of AQP4 homologue AQP0, reconstituted in a 2D lattice with 6.4 nm periodicity (cropped from Fotiadis *et al.*, 2000), on the same scale as (b), for comparison.